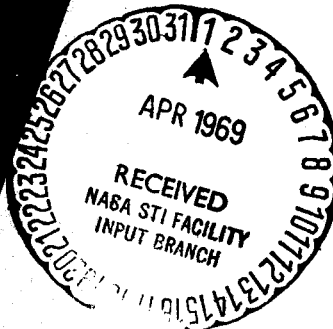N69 25369

NASA-CR-98420

N.T.

CASE FILE COPY

SOLAR FLARE RADIATION PROTECTION REQUIREMENTS
FOR PASSIVE AND ACTIVE SHIELDS

Francis W. French

RESEARCH REPORT 331
Contract NAS 8 - 21392
March 1969

prepared for

NATIONAL AERONAUTICS AND SPACE ADMINISTRATION
GEORGE C. MARSHALL SPACE FLIGHT CENTER
Huntsville, Alabama

AVCO EVERETT RESEARCH LABORATORY
A DIVISION OF AVCO CORPORATION

SOLAR FLARE RADIATION PROTECTION REQUIREMENTS
FOR PASSIVE AND ACTIVE SHIELDS*

by

Francis W. French

AVCO EVERETT RESEARCH LABORATORY
a division of
AVCO CORPORATION
Everett, Massachusetts

March 1969

Contract NAS 8-21392

prepared for

NATIONAL AERONAUTICS AND SPACE ADMINISTRATION
GEORGE C. MARSHALL SPACE FLIGHT CENTER
Huntsville, Alabama

ABSTRACT

The degree of protection from solar flare radiations required by astronauts on interplanetary flights is investigated if the protection is provided by: (a) passive means (bulk shielding), and (b) active means (Plasma Radiation Shielding). Anticipated solar flare radiation environments postulated in several recent studies are examined and found to fall into two general categories. Radiobiological tolerance criteria based on early skin and blood-forming organ responses are discussed. Several approaches to selecting a mission radiation exposure criterion are considered, and example criteria suggested for illustrative purposes. Curves are presented of dose vs shield thickness and Plasma Radiation Shield voltage, with probability of exceeding a given dose as a parameter. These curves are used to obtain requirements for the two types of shielding. Results are compared on several bases.

TABLE OF CONTENTS

I. INTRODUCTION AND SUMMARY

The hazards posed to astronauts on deep space missions by ionizing radiations need no elaboration here. Protection can be afforded in two basic ways which may be categorized as "passive" or "active" methods. Passive methods consist of placing radiation-absorbing material around the cabin to reduce the incident radiation to acceptable levels. The sizeable thicknesses (and weight) required of such material usually dictate that only a minimum-size "storm cellar" be protected. Active concepts utilize electrostatic and/or magnetic forces to deflect charged-particle radiations. Several such concepts have been advanced but investigation has shown that the only one that combines the promises of reduced shielding weight and elimination of the disadvantages of a storm cellar with reasonable expectation of success is the Plasma Radiation Shield (PRS). [1,2]

This study investigates the space radiation shielding requirements for manned, deep space missions if the protection is provided by either passive or active (PRS) systems. A limited comparison is made between the requirements for the two types of systems, and the data is provided for broader and more meaningful comparisons as PRS technology is advanced.

The space radiations considered in this study are those bursts of protons and alpha particles that are associated with flares on the solar disc (hereafter called for brevity, solar flare radiations). Radiations of galactic origins as well as those associated with the Van Allen Belt are not considered-- both because their inclusion would cloud the basic comparisons that are made and because they are generally of secondary importance.

Section II considers solar flare radiation environments as postulated in several recent studies. The end-product of this portion of the study is to relate shielding parameter (in terms of bulk thickness or PRS voltage) to dose received by the astronauts on a typical mission, with various probabilities of exceeding these levels as parameters. Section III relates radiation dose level at skin and blood-forming organs to radiobiological damage. Mission exposure criteria that relate allowable radiation dose levels to probability of exceeding these levels are considered in Section IV, and are utilized to determine shielding requirements for both types of shielding systems.

II. ANTICIPATED SOLAR FLARE ENVIRONMENT

Background

Predictions of the space radiation environment associated with solar flare events are, of necessity, based on previous observations of these phenomena. These observations were mainly carried out during the last solar cycle. As time goes by, the level of confidence in these predictions should increase as more and better in situ observations are made by satellites and space probes. Also, at some time in the future, solar phenomena may be sufficiently understood so that meaningful solar radiation "weather forecasts" can be made sufficiently far in advance to affect the planning of long-duration, interplanetary missions. However, the attainment of such understanding is not in sight at the present time, and present-day space mission planners must rely on existing observational data to postulate anticipated radiation environments for future interplanetary missions.

The occurrence of flares, as well as their flux intensities and spectral characteristics apparently have random distributions (at least in a given portion of the solar cycle). Thus, current predictions of anticipated solar flare environments are generally based on probabilistic considerations. Questions of which distribution functions (for flare occurrence, flux intensity, and spectral characteristics) are most appropriate for predicting future solar flare environments are quite subjective. Therefore, the environments postulated by a given investigator are colored by his interpretation of the existing data, and arguments as to the "correctness" of one model environment as opposed to another are largely nugatory.

Objectives and Assumptions

This portion of the study considers model solar flare radiation environments as postulated in several studies, and interprets these in terms of solid shield thickness and PRS voltage. In order to meet this objective, it is necessary to have a common basis of comparison.

The mission duration selected for the example is 1-1/2 years, which is fairly representative of current thinking on durations for manned Mars missions. It is assumed that the model solar flare environment encountered is that occuring at about 1 AU, although it is realized (eg, Ref. 3) that the varying solar distance on interplanetary trips could modify this environment. Because it represents a more severe case, it is assumed that the mission occurs in the upper half of a future solar cycle. Although it has been suggested that the next few solar cycles will probably contain fewer flares than the last (solar cycle 19), no assumptions are made in this regard, and the analyses are carried out on the basis that the flare frequency in

Solar Cycle 19 was typical of all others. The time-variations of individual flares are ignored and only the time-integrated characteristics are considered. The particle flux is assumed to be isotropic and no short-term prediction capability is assumed. For ease of comparison of results, it is assumed that for the passive shielding case the astronauts are shielded by a spherical aluminum shield (although it is realized that this material is far from being an optimum one). Radiobiological doses from the flares are calculated at two body locations--the skin and the blood-forming organs. The dose for the former is calculated at about 0.1 mm below the body's surface, and for the latter at 4 to 5 cm below the surface. These two dose locations are felt to represent, in a sense, two extremes and it has been shown that each of them is important under certain circumstances. In calculating the radio-biological dose, production of secondary radiations will (generally) be neglected. It has been shown (eg, Refs. 4, 5) that the dose contributions from secondaries are generally relatively small for shielding thicknesses and flare spectra of interest.

The approach used by a particular investigator in formulating a model environment will be utilized to obtain results in a common form. The selected form for comparison is that of curves of radiobiological dose (to skin and blood-forming organs) vs aluminum shield thickness and PRS voltage, with probabilities (0.1%, 1%, and 10%) of exceeding that dose on a 1-1/2 year mission as parameters. As discussed in subsequent sections, these curves can be used in conjunction with a given radiobiological dose criterion to determine shielding requirements as a function of probability that the given criterion is not exceeded.

Passive Shielding

Differences in predicted solar flare environment, and consequently in shielding requirements, can mainly be attributed to differences in assumed distribution functions. There is apparently no correlation between the number and intensity of individual flares during a given period. Therefore, although it is likely that the number of flares during the next several solar cycles will not exceed that in Solar Cycle 19, one may argue that there is a finite probability of the occurrence of a flare more intense than any seen to date. Whether or not one accepts this premise can lead to markedly different shielding requirements. This point has been mentioned by Modisette et al,[6] but will be elaborated on and quantified in the ensuing discussions.

An example of the results of the assumption that astronauts will encounter no solar flare more severe than those occuring during Solar Cycle 19 is afforded in the work of Webber.[7] For each solar flare observed in the years 1956 through 1962, Webber calculates and tabulates the dose (both at skin and blood-forming organ depths) behind various thicknesses of aluminum shielding. He then considers missions of 30-and 60-day durations to start on each day during this seven year period, and calculates the doses that would have been received on each mission. He uses these data to obtain curves of dose vs probability of exceeding that dose for 3 aluminum thicknesses and for the two mission durations which he considered (see Figs. 21 and 22 of Ref. 7). Webber follows an analogous procedure for longer missions and obtains curves of mission-integrated flux (rather

than dose) vs probability of exceeding that flux for mission durations of 3, 6, 14 and 24 months (see Fig. 23 of Ref. 7). Although the results in these figures apply to Solar Cycle 19, it is implied that they can be used as a model environment for future space missions. Webber's results, as they stand, cannot be applied directly for comparison with similar works since the results of his Figs. 21 and 22 are for short-duration missions (1 and 2 vs 18 months), and the results of his Fig. 23 are in terms of flux rather than dose. However, it was found that some simple considerations, which will now be described, allow these results to be put into a canonical form that is suitable for comparison.

The data of Table 8 of Ref. 7 is used to plot, in Fig. 1, a histogram of the dose that would be received from solar flares in the period 1956 through 1962. Two types of dose are considered for illustrative purposes: skin dose behind 5 gm/cm^2 and 4-cm depth dose behind 4 gm/cm^2 of aluminum. Other amounts of shielding would, of course, give different values in Fig. 1 but would not change the conclusions which will be reached. (It should be noted in Fig. 1 that the three event-sequence in July 1959 and the three event-sequence in November 1960 are both treated as single events). Inspection of Fig. 1 shows that of all the 50 solar flares that occurred in the time period of interest, there were only a few that were really significant in delivering skin or 4-cm doses behind shield thicknesses of interest. For a 1-1/2 year mission, the largest dose is accumulated when the mission encounters the July 10-16, 1959 and the November 12-20, 1960 flare sequences. The total dose is then (neglecting several small events in between) 204 + 156 = 360 rad. The time period that just covers these events is 498 days, as compared to the total mission duration of 1-1/2 years = 547.5 days. If one imagines a new mission started on every day from January 1, 1956 to December 31, 1962, there are 2557 missions that could be flown. Of these, about 547 - 498 = 49 or 49/2557 = 1.9% will encounter 360 rad.

The next worst class of missions would include the May 10, 1959 event and the July 10-16, 1959 sequence, which would give a total dose (including a small event in between) of 55 + 5 + 204 = 264 rad. In this period there are 67 days and thus there will be 547 - 67 = 480 missions or 480/2557 = 18.8% that will encounter 264 rad. However, as stated earlier we are interested in the doses that correspond to given probabilities (0.1%, 1%, 10%) of encounter or, what amounts to the same thing, the doses that correspond to an encounter in given percentages of missions. Since we have estimates of the doses corresponding to 1.9% and 18.8% probabilities, the doses for 1% and 10% probabilities can be found if one assumes a distribution function and in the first case extrapolates and in the second interpolates. A log-normal distribution was assumed and the doses corresponding to 1% and 10% probabilities were obtained graphically; it was felt that the data did not warrant extrapolation to the 0.1% probability case.

It should be remembered that the above procedure was described in terms of the skin dose behind 5 gm/cm^2 of aluminum. One can follow an analogous procedure in terms of the skin dose (or the 4-cm dose) behind other shield thicknesses, and obtain values of skin and 4-cm dose that can be expected to be exceeded 1% and 10% of the time behind various shield
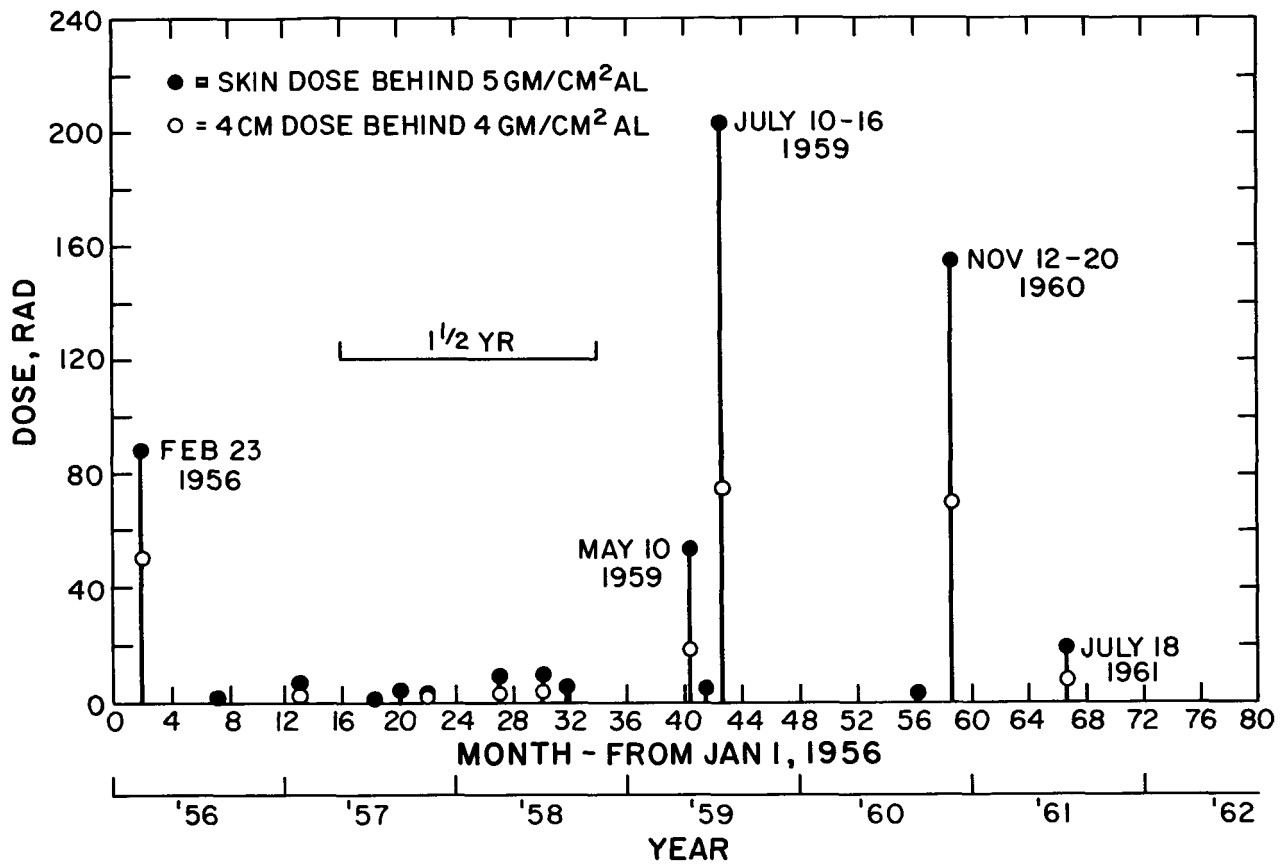
Fig. 1   Dose History for Solar Cycle 19

-6-

thicknesses for 1-1/2 year missions. This was carried out and the results plotted as curves of dose vs shield thickness for various probabilities of occurrence in Figs. 2 and 3.

Burrell et al. [8] uses flare size and number distributions that are based on the distributions of Solar Cycle 19 flares. He calculates skin and 5-cm depth doses for the significant flares in the 1956-1962 time period and the results in his Table III are very close to those in Webber's [7] Table 8, when allowance is made for the difference in blood-forming organ average depth that each assumed. Other assumptions made in Reference 8 were that: an event was assumed to consist of one, two or three flares in the period of a week in the same ratios as observed in Solar Cycle 19; flares making up an event were of the same size; and the events were distributed randomly over the six-year active period. Using these assumptions, the authors developed a Monte Carlo model and obtained weekly doses by random sampling. Cumulative probability distributions were formed for 2 and 52-week missions and several shielding thicknesses, and are plotted in Figs. 19a and 19b of Ref. 8. These results are also given in Figs. 20a and 20b of Ref. 8 in the form of skin (only) dose vs shielding thickness curves for probabilities of 0.1%, 1%, 5% and 10%. The data presented in Fig. 20b of Ref. 8 is close to required form, except that the mission duration is 1 year instead of 1-1/2 years. The data is modified for the 1-1/2 year missions by an appropriate correction suggested by Snyder, [9] which is discussed below. Final results are plotted in Figs. 2a, 2b, and 2c.

Another model solar flare environment that is also based on the assumption that future solar cycles will include no flares more intense that those observed in Solar Cycle 19 is suggested by Hilberg. [10] Missions at both solar minimum and solar maximum are considered, but only the former will be discussed here. Hilberg assumes that the probability of encountering major solar flare events can be obtained from a Poisson distribution with an anticipated frequency of one per year. The "standard" large event is chosen such that it produces a 25 rem depth dose (presumably at 4 or 5 cm) behind 10 gm/cm^2 of aluminum and 40 rem behind 5 gm/cm^2. Curves are presented in Fig. 3 of Ref. 10 of (presumably depth) dose vs probability of receiving a greater dose on a one year mission for two shielding thicknesses, 5 and 10 gm/cm^2. The dose values in this figure include a contribution of from 15 to 17.5 rem from galactic cosmic rays.

As they stand, Hilberg's results cannot be directly put in the canonical form for comparison because they are for a one, rather than a 1-1/2, year mission and because they do not contain enough information on the variation of dose with shield thickness. Hilberg's method, was, however, used to obtain the desired results in the following manner.

A Poisson distribution was assumed for the flare occurrence frequency during the 1-1/2 year mission, and probabilities of encountering none or at least 1, 2, ... N, events were calculated. These results are shown in Table 1.
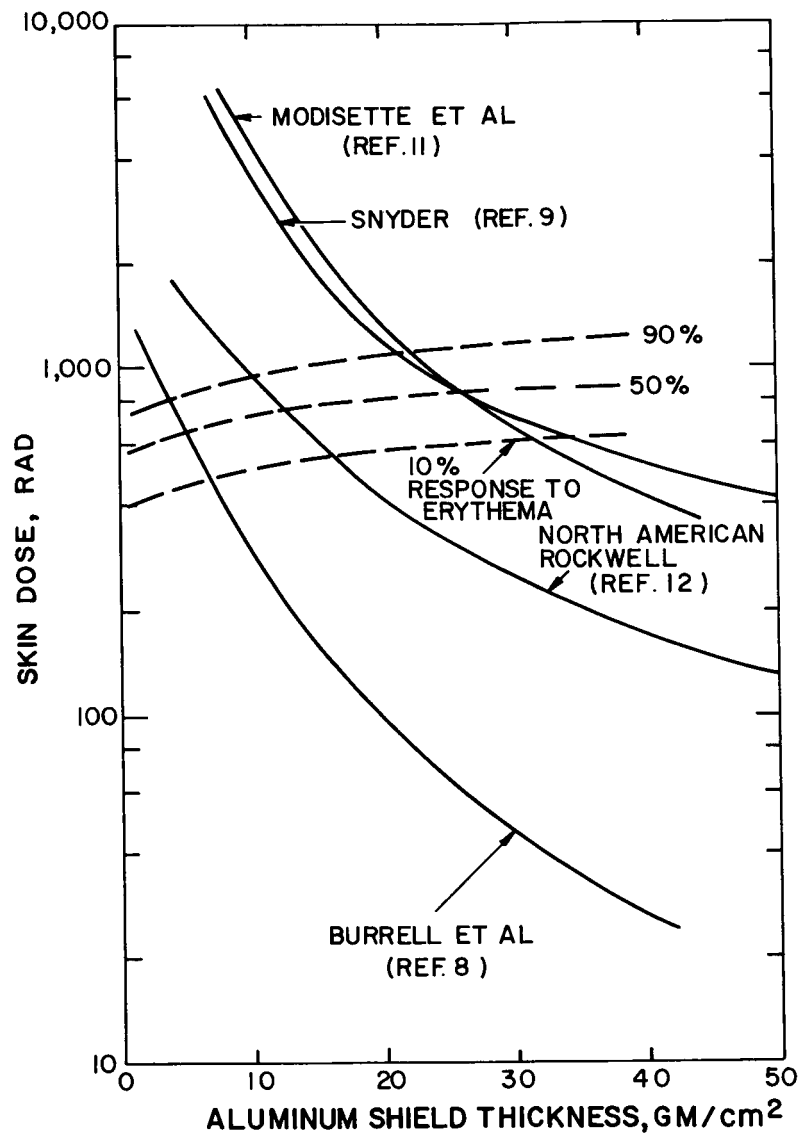
Fig. 2a   Skin Dose vs Aluminum Shield Thickness Required for Various
Probabilities of Exceeding a Given Dose (a) p = 0.1%
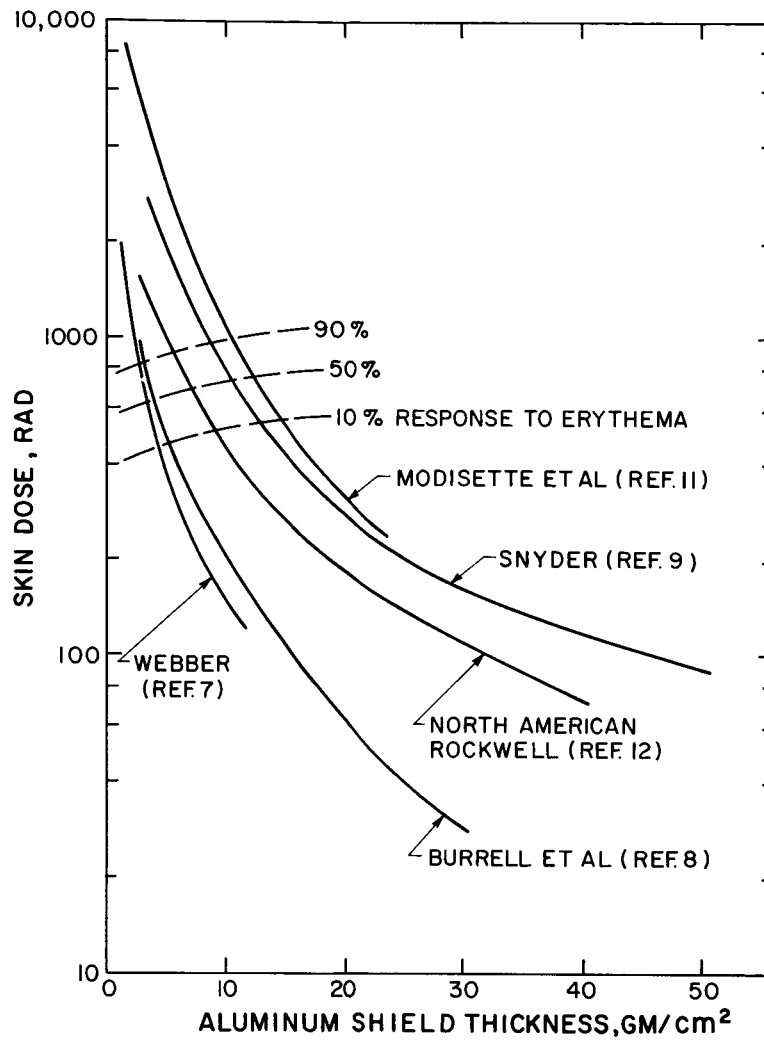
Fig. 2b   Skin Dose vs Aluminum Shield Thickness Required for Various
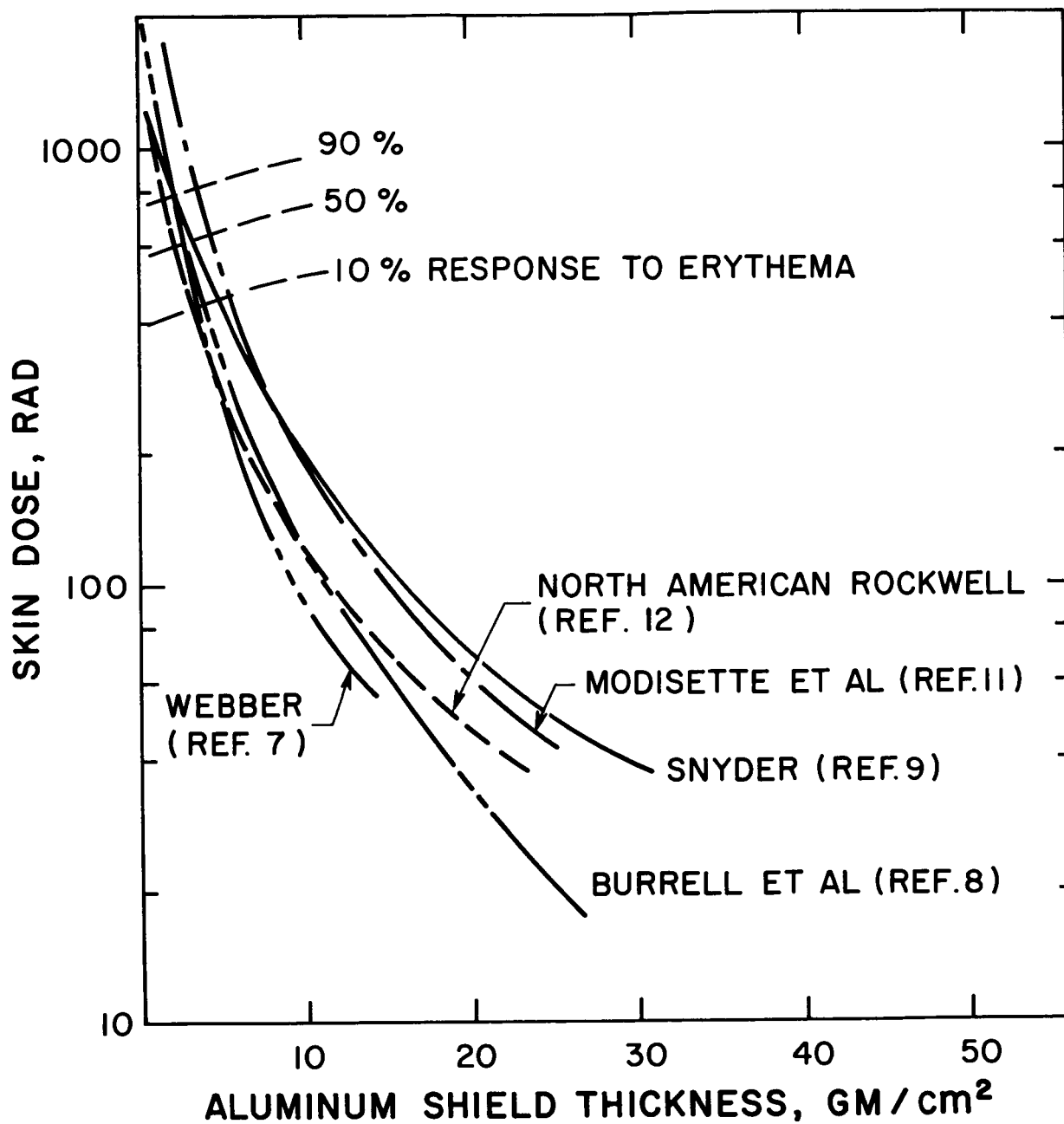Probabilities of Exceeding a Given Dose (b) p = 1. 0%

Fig. 2c   Skin Dose vs Aluminum Shield Thickness Required for Various
Probabilities of Exceeding a Given Dose (c) p = 10%

TABLE 1

Probability p of Encountering N Events

N	p, %
0	22. 3
at least 1	77. 7
at least 2	44. 3
at least 3	19. 2
at least 4	6. 7
at least 5	1. 9
at least 6	0. 4
at least 7	0. 1

Use of Table 1 then allows calculation of depth dose from Hilberg's standard flare for the probability values given in Table 1 and for the 5 and 10 gm/cm^2 thicknesses --eg. , behind a 5 gm/cm^2 shield, there is a 6.7% probability of receiving a dose greater than $4 \times 50 = 160$ rem. However, for the sake of comparison, we are interested in specific values of probability -- 10%, 1%, and 0.1%. Therefore, the values in Table 1 were plotted, a smooth curve drawn between the points, and interpolation performed to obtain the "number of events" corresponding to the desired probability values. In this way it was possible to get depth dose values for shielding thicknesses of 5 and 10 gm/cm^2 and the 3 probability values. However, to plot dose vs thickness curves, it is necessary to have more than 2 points per curve so further interpretation of Hilberg's work was required. Although it was not stated by Hilberg, it was noted that the dose distribution characteristics of his "standard" event were similar to the February 23, 1956 flare. Thus it was assumed that his "standard" event had the same spectral distribution, but 83% of the integrated flux of the February 23, 1956 event. In this manner, the depth doses behind 5 and 10 gm/cm^2 were brought into coincidence for both events, and Webber's dose calculations (Table 8 of Ref. 7) could be used to calculate dose values behind other shield thicknesses. The resulting depth dose vs thickness curves are shown in Figs. 3a, 3b, and 3c.

Fig. 3a   Blood-Forming Organ Dose vs Aluminum Shield Thickness Required for Various Probabilities of Exceeding a Given Dose (a) p = 0.1%

B 3027
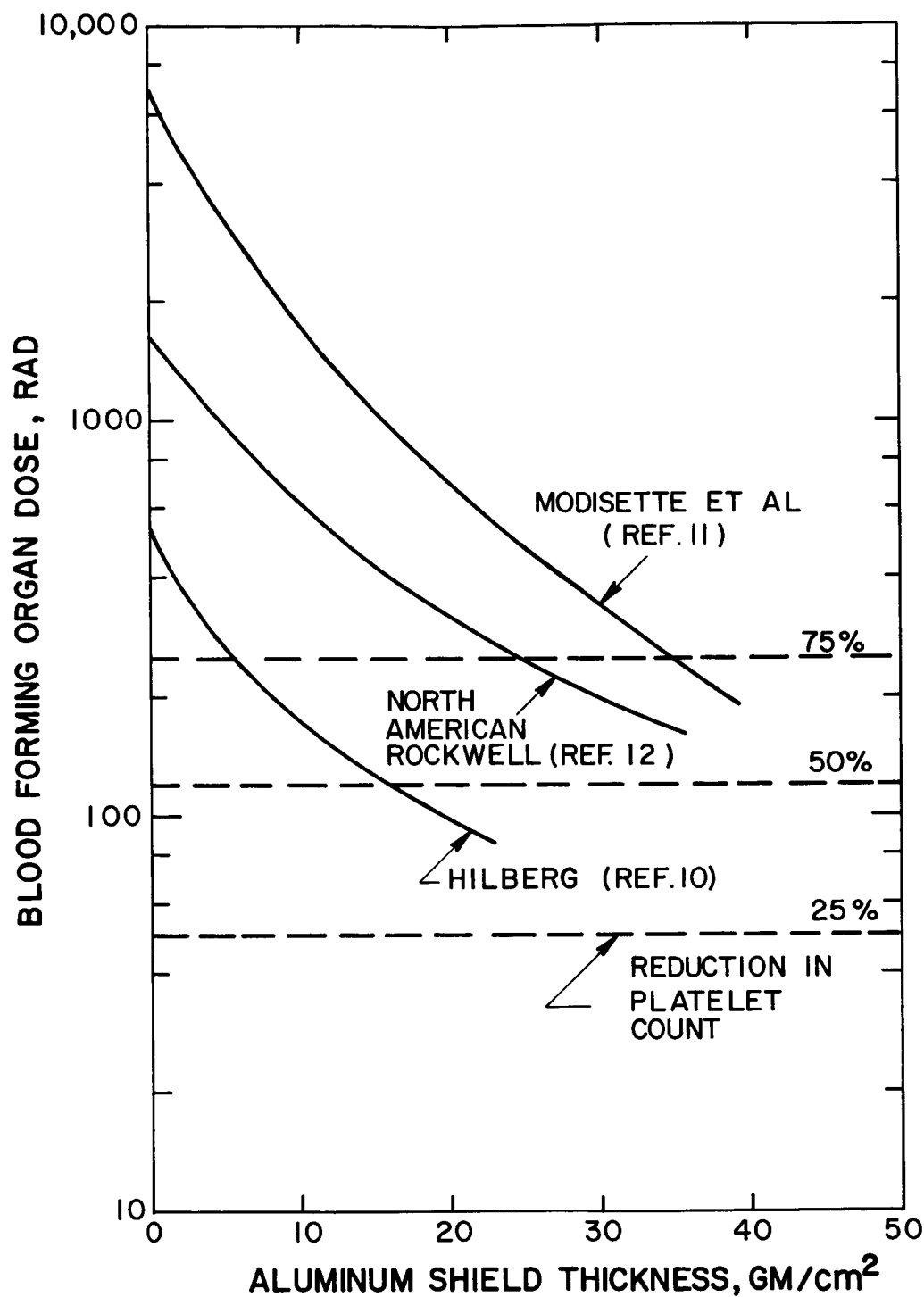
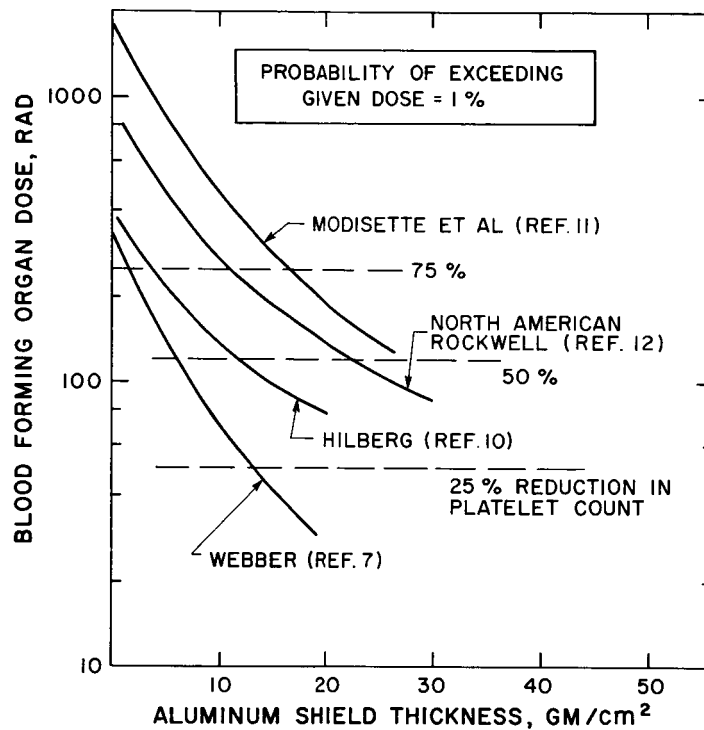Fig. 3b   Blood-Forming Organ Dose vs Aluminum Shield Thickness Required for Various Probabilities of Exceeding a Given Dose
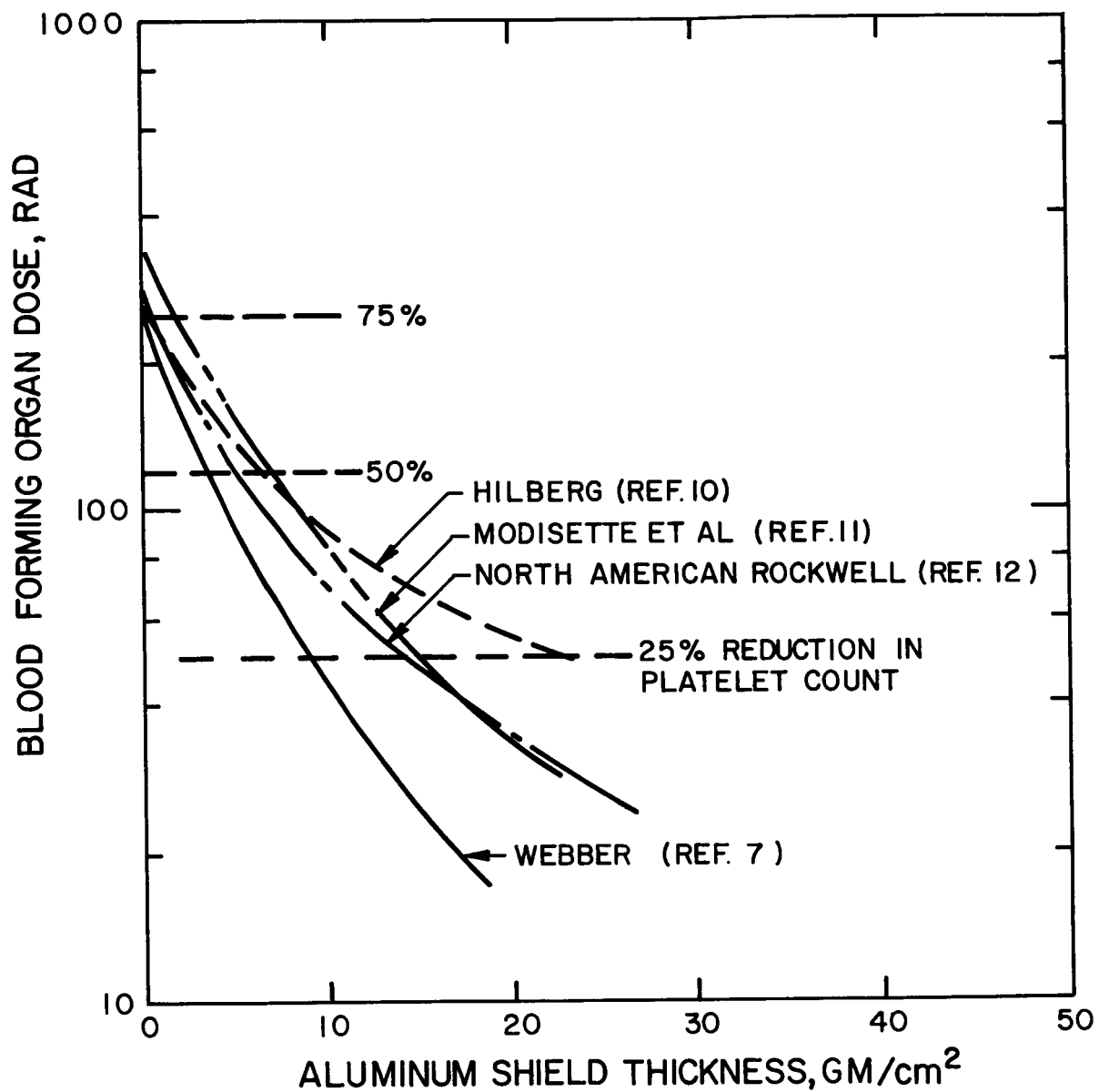(b) p = 1. 0%

Fig. 3c   Blood-Forming Organ Dose vs Aluminum Shield Thickness Required for Various Probabilities of Exceeding a Given Dose
(c) p = 10%

The second approach, that of assuming there is a finite possibility of encountering a solar flare (or flares) more intense then anything seen in Solar Cycle 19, is typified by the environments proposed by Modisette et al. [11] and Snyder. [9] It is assumed in Ref. 11 that the time-integrated spectra of all solar flare events can be represented by an exponential rigidity relation of the form:

$$F\ (\ > E) =\ G \exp\ (- P(E)/P_o) \qquad (1)$$

Where G is the event flux parameter, $P(E)$ is the magnetic regidity, E is the proton energy, P_o is the characteristic rigidity, and F (>E) the integrat-ed flux of protons with energy greater than E. Values of integrated flux greater than 30 and 100 MeV, and of characteristic rigidities, are tabulated for the major events during Solar Cycle 19. For a given mission duration, Modisette et al. consider each day in the period 1956 through 1961 to start a new mission, and use the tabulated flux values to obtain the total number of protons, N, encountered during each mission. The distribution of number of protons are determined for those missions which do encounter flares, and it is found that the distribution is log-normal. These distributions are shown in Figs. 2a through 2d of Ref. 11 for 1, 2, 52, and 104-week missions. The data in these figures are cross-plotted in Figs. 3a and 3b of Ref. 11 to yield curves that show the variation of time-integrated proton flux with mission length for 4 probability levels. It is also shown that it is very likely that the major portion of the total flux encountered (and therefore the total dose received) during a mission will occur from one or a few large events.

Although no dose calculations were reported in Ref. 11, it was suggested that a P_o value of 97 MV be used for calculating the dose received during a mission since this value is the mean of values tabulated for events occurring from 1956 through 1961. It is also shown that the choice of a particular value of P_o has only a secondary influence on total mission dose. An advantage to the formulation suggested by Modisette et al. is that only one set of calculations need be performed to obtain a dose vs shielding thickness curve, using the reference spectrum and a reference integrated flux value (say 10^9 protons/cm^2 with energies greater than 30 MeV). For a given thickness, doses resulting from encounters with a greater or lesser number of protons can then be obtained by ratioing the flux values. At this point it may be noted that the formulation of Ref. 11 allows the possibility of receiving a large dose due to the finite probability of encountering a total number of protons much larger than would have been encountered any time during Solar Cycle 19.

The data presented in Fig. 3b of Ref. 11 was used to obtain the number of protons that would be encountered with probabilities of 0.1%, 1% and 10% on a 1-1/2 year mission. Calculations were performed, using the reference event, to obtain skin and blood forming organ doses behind various thicknesses of aluminum shielding. The total number of protons encountered during the mission, as obtained from Fig. 3b of Ref. 11, was

then used to obtain the total dose received during the mission. Results are plotted in Figs. 2a to 2c and Figs. 3a to 3c.

Snyder[9] used flux and spectra compiled by Modisette et al.[11] for 54 significant solar proton events in the period 1956 through 1961 as input data for shielding calculations. For these calculations a computer code was used which included the effects of secondary radiations and yielded an output in terms of skin dose in rem behind various amounts of aluminum shielding for each solar flare. For a given shield thickness, the doses from the events are shown to follow a log-normal probability distribution (Fig. 1 of Ref. 9). The difference in flare frequency between solar maximum and minumum is noted; 9 flares/year are assumed as average for solar maximum and 0.6/year for solar minimum. The occurrence of other numbers of flares per year is assumed governed by what is effectively a Poisson probability distribution, and, for instance, there is a 0.01% chance of encountering 22 flares per year.

A sample of 10,000 missions is considered and the Poisson distribution used to calculate the number of missions in which 0, 1, 2... solar events occurred. By means of random sampling of the dose per distribution and subsequent summing, the total dose for each mission (for a given shield thickness) was computed. After arranging the mission doses in order of size, it was possible to obtain the mission doses that would be exceeding in 0.1%, 1%, 10% and 50% of the missions. Varying the shield thickness then allowed construction of skin dose vs shield thickness curves with probability of exceeding a given dose as a parameter. Snyder presents such curves (Figs. 2 and 3 of Ref. 9) for one-year missions at solar maximum and minimum, based on the 9 and 0.6 flares/year observed during Solar Cycle 19. He also allows for the possibility that the number of flares observed at the maximum of Solar Cycle 19 were considerably higher than for the "average" solar cycle and presents appropriate dose vs thickness curves. Snyder also presents dose correction curves that allow the construction of dose vs thickness curves for mission durations other than one year. These latter curves were used in conjunction with Snyder's Fig. 3 to obtain the curves for the 1-1/2 year mission that are shown in Figs. 2a to 2c. It should be noted that although Snyder's results were given in terms of rem, they are plotted in Figs. 2a to 2c in terms of rad, the implication being that the Quality Factor for these radiations is unity. Although it is recognized that the Quality Factor for early skin response is somewhat higher (discussed later in this paper), this approximation was necessary as it was not possible to extract the rad dose from Snyder's data in Ref. 9.

In a recent North American Rockwell report,[12] analytic expressions are developed to predict the shielding requirements for manned interplanetary flights. This report is interesting in that the analytic expression proposed for relating total mission flux to probability of exceeding that flux plots between the analogous curves of Webber[7] and those of Modisette et al.[11] This expression is (in the nomenclature of Ref. 12):

$$p\,(t) = \exp\left[-B(\int\phi/t)^{\eta}\right] \qquad (2)$$

where p = probability of exceeding a given flux on a mission of duration t, $\int\phi$ is the mission-integrated proton flux > 30 MeV, η is a constant and B is a factor that varies sinusoidally from solar maximum to a solar minimum. It is assumed that for each event, and consequently for the sum of events during a mission, the spectrum can be represented as

$$\int\phi\,(E > E_o) = A/E_o^{1.55} \qquad (3)$$

where $\int\phi\,(E > E_o)$ is the proton flux of energy greater than E_o and A is a constant. Using appropriate analytic relations for range-energy and for flux-to-dose conversion, it is then possible to evolve an analytic expression that relates dose, probability of receiving that dose, mission duration, and shield thickness. This is carried out in Ref. 12 and the following expression which includes the dose contribution from alpha particles, and which has been specialized for solar maximum and a 1 AU spacecraft-sun distance, results:

$$X = 26\left[t/D^X_{p\,+\,\alpha}\right]^{0.77}\left[-\ln p\,(t)/2.5\right]^{1.54} \qquad (4)$$

where X is the aluminum shield thickness in gm/cm^2, t is the mission duration in weeks, $D^X_{p\,+\,\alpha}$ is the point dose in rad due to protons plus alpha particles behind shield thickness X. It is assumed that point dose is related to skin and blood-forming organ dose in the following manner:

Skin Dose behind X gm/cm^2 Al =

$$\frac{1}{2}\left[\text{Point Dose behind X } gm/cm^2 Al\right] \qquad (5a)$$

Blood-Forming Organ Dose behnid X gm/cm^2 Al =

$$\frac{1}{2}\left[\text{Point Dose behind (X + 5) } gm/cm^2 Al\right] \qquad (5b)$$

It might be noted that the multiplying factors on the right hand sides of Eqs. (5a) and (5b) are actually dependent on both shield thickness and on "hardness" of the flare spectra; for example, French and Hansen[4] give typical values for the factor in Eq. (5a) between 0.56 and 0.74 for some flares and shield thicknesses of interest. Also, it might be observed that

an implication in Eq. (5b) is that 5 gm/cm^2 of aluminum has the equivalent stopping power as 5 gm/cm^2 of tissue, an approximation which is not particularly accurate.

Equation (4) was used in conjunction with Eqs. (5a) and (5b) to calculate skin and blood-forming organ doses for the 1-1/2 year mission. The results obtained are shown in Figs. 2a to 2c and 3a to 3c.

A few conclusions may be drawn from the results as presented in Figs. 2 and 3. First, the differnece in shielding requirements that results from the two basic premises is indicated. Modisette et al.[11] and Snyder[9] on the one hand, assume that events more intense than any previously observed can conceivably occur (a "pessimistic" - type environment). The shielding requirements resulting from this assumption are generally more severe than those resulting from the assumption that no events more severe than those previously observed will occur (an "optimistic" - type environment). The latter assumption was made by Webber,[7] Burrell et al.,[8] and Hilberg.[10] North American Rockwell[12] used an assumption for the environment between these extremes and, as expected, their shielding requirement curves generally lay between the other two sets. Inspection of Figs. 2 and 3 show that the differences between the results of the two approaches are most pronounced at low probabilities (eg., 0.1%), and that the curves tend to coalesce at higher probabilities (eg.,10%), an outcome that could be anticipated from the nature of the basic assumptions. Also of interest in Fig. 2 is the close agreement of the results of Modisette et al.[11] and Snyder,[9] in spite of different methods of attacking the problem. In passing, it might be noted that at large shielding thicknesses (i.e., greater than about 20 gm/cm^2), Snyder's results may be more accurate than others in the sense that his shielding calculations include the effects of secondary radiations in a thickness regime where they can become significant. Also, the rem-rad approximation that was used in plotting Snyder's results should be recalled.

Plasma Radiation Shielding

The Plasma Radiation Shield concept has been described in Ref. 1 and its application to manned spacecraft in Ref. 2. Very briefly, the Plasma Radiation Shield is an electrostatic shield with a shielding voltage maintained between the positively charged spacecraft and a surrounding cloud of free electrons. The cloud of electrons is held in place by a magnetic field, and the outer edge of the cloud is at potential of free space. The charges on the spacecraft and the electron cloud are equal and opposite, so that the arrangement can be considered as a capacitor. As a consequence of this arrangement, a positively charged proton will be repelled by the spacecraft if its energy E_0 is less than the spacecraft's potential, V. If its energy is initially greater than V, it will penetrate the shield with an energy $E_1 = E_0 - V$. Also, particles having an energy just greater than V in free space will be strongly deflected by the electric field, and can only penetrate it if their initial motion is accurately parallel to some electric field line. An estimate of the strength of this effect is that the flux of particles of energy $E_0 (> V)$ is reduced by the factor $(E_0 - V)/E_0$ in passing through the field.

This factor is strictly correct for simple geometries and is probably at least representative for more complicated ones. In general, it emphasizes the deflection, or scattering phenomenon, for particles with free space energy E_0 just greater than V. When E_0 is much greater than V, the deflection is insignificant, and the factor goes to unity. If ϕ (E) is the differential flux distribution function, the fluxes inside and outside the PRS are related as follows:

$$\phi (E_1) = \frac{E_0 - V}{E_0} \phi (E_0) = \frac{E_1}{E_1 + V} \phi (E_1 + V) \qquad (6)$$

If the free space integral spectrum has the exponential rigidity form given by (Eq. 1), the corresponding differential spectrum in terms of energy is then

$$\phi (E_0) \frac{G}{P_o q} = \left[\frac{E_0 + M}{\sqrt{E_0^2 + 2ME_0}} \right] \times \exp - \left(\frac{\sqrt{E_0^2 + 2ME_0}}{P_o q} \right) \qquad (7)$$

where q is the particle charge (=1 for protons), and M is the rest mass energy (= 938 MeV for protons). Then for a given integral spectrum, as specified by values of G and P_o in Eq. (1), Eqs. (6) and (7) may be used to obtain the differential spectrum inside the PRS with a given voltage V. Use of a suitable flux-to-dose conversion then allows computation of the dose absorbed by the astronauts inside the PRS; (in carrying out the calculations described below, a conversion factor was selected that gave dose results for the solid shielding case that agreed with those of Webber[7] and Burrell[8]). This computational procedure was used to generate curves of dose vs PRS voltage with probability of exceeding a given dose as a parameter. These curves were obtained for both representative "pessimistic" and "optimistic" solar flare environments; these environments were evolved from those described in the previous subsection in the following manner:

The model environment of Modisette et al.[11] was selected as being typical of the pessimistic-type solar flare environment. As was discussed previously, this reference assumes that the spectrum of a typical flare can be represented by Eq. (1) with P_o = 97 MV. A value of integrated flux of 10^9 protons/cm^2 above 30 MeV was arbitrarily selected (being a typical value for a large event), and the computational procedure described above was used to obtain curves of skin and BFO dose vs PRS voltage for this "typcial" flare. Fig. 3b of Ref. 11 presents information that relates mission-integrated flux to probability of encountering a given flux for the 1-1/2 year mission. Since the characteristic rigidity (P_o) is assumed constant, the mission-integrated dose is proportional to the mission-integrated flux. Thus the relations between dose and voltage, and between

flux and probability, can be combined to yield curves of dose vs voltage with probability of exceeding a given dose as a parameter. Such curves, which are analogous to those in Figs. 2 and 3 for the passive shielding case, are shown in Figs. 4 and 5.

It might be noted that the BFO dose curves in Fig. 5 are slightly concave downward. This seemingly-anomalous behavior can be explained by the choice of abscissa; if voltage is converted into "equivalent" solid shield thickness, the curves will take the familiar concave-upward form.

The model environment of Hilberg[10] was selected as being representative of the optimistic-type solar flare environment. As was discussed previously, the typical solar flare event assumed in Ref. 10 had characteristics similar to the February 23, 1956 flare. It is assumed that the spectrum of this event can be adequately represented by an exponential rigidity type relation (Eq. 1) with $P_o = 195$ MV and $G = 2.83 \times 10^9$ proton/cm^2. Calculations are then performed, as described in the previous paragraph, to obtain curves of dose vs PRS voltage for this event. With the probability of encountering a stated number of solar flare events given by the Poisson distribution, it is possible to obtain curves of dose vs PRS voltage with probability again as a parameter. These curves are shown in Figs. 6 and 7.
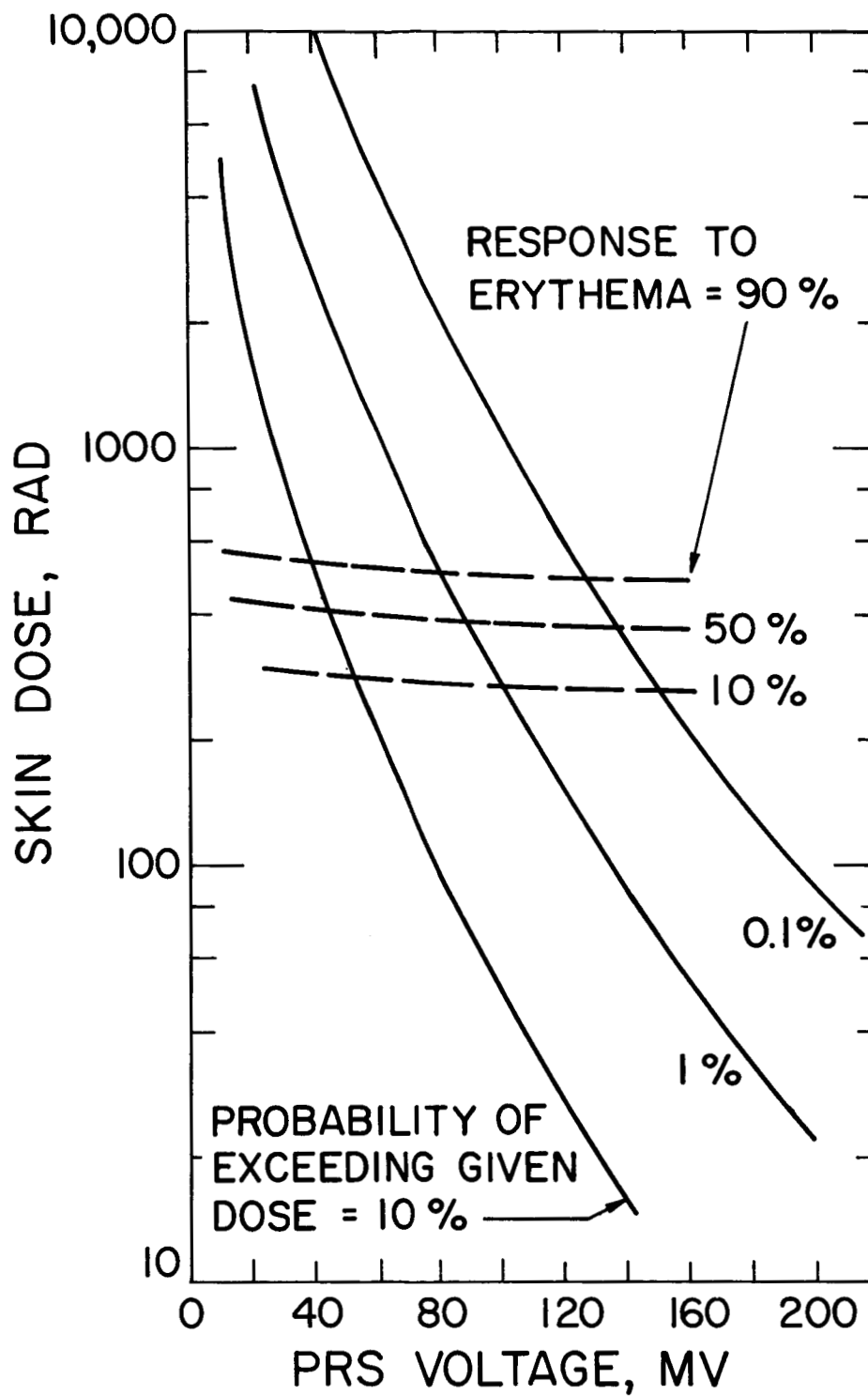
Fig. 4   Skin Dose vs PRS Voltage Required for Various Probabilities
of Exceeding a Given Dose -- "Pessimistic" Environment
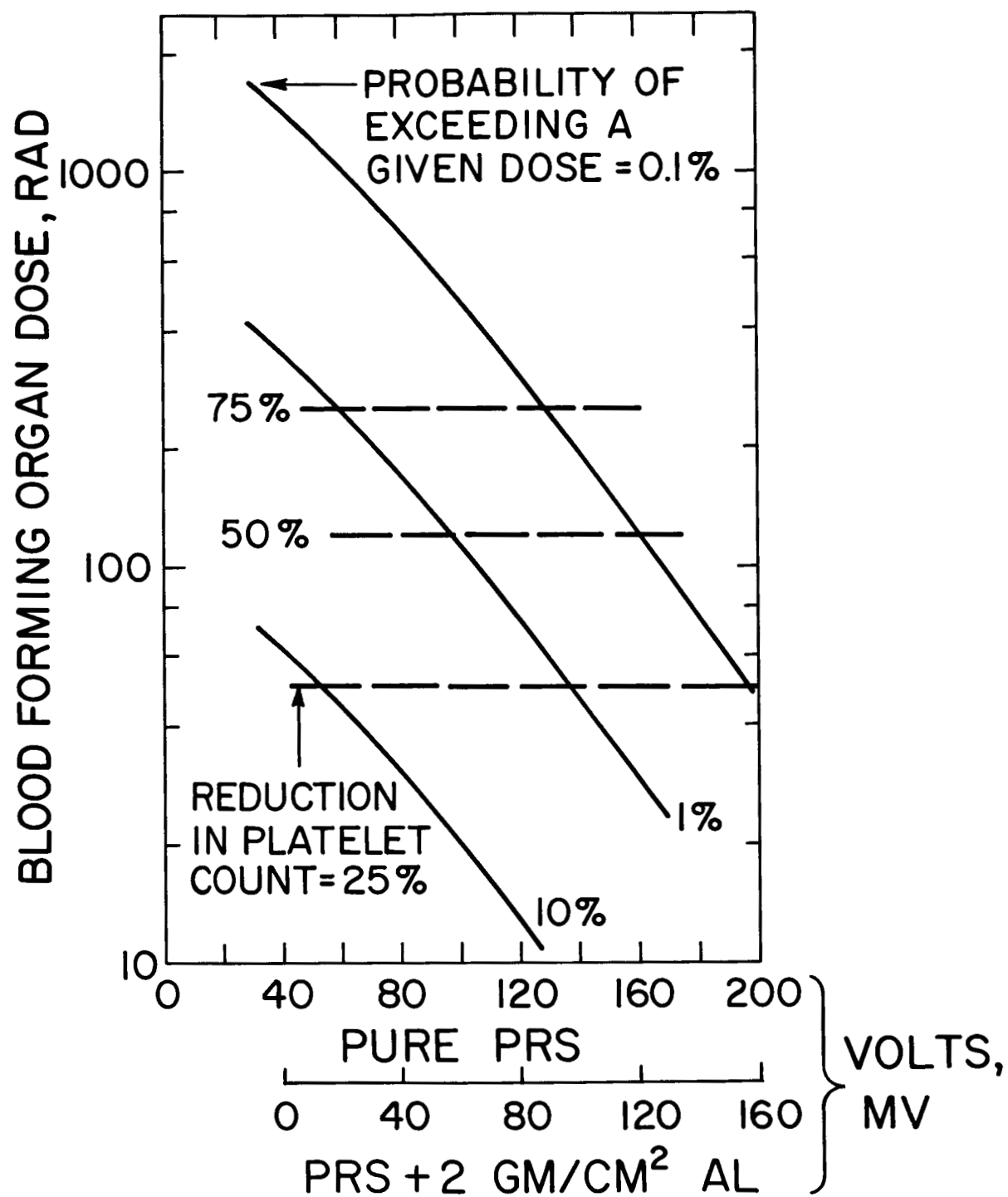
B 3398

Fig. 5   Blood-Forming Organ Dose vs PRS Voltage Required for Various Probabilities of Exceeding a Given Dose -- "Pessimistic" Environment
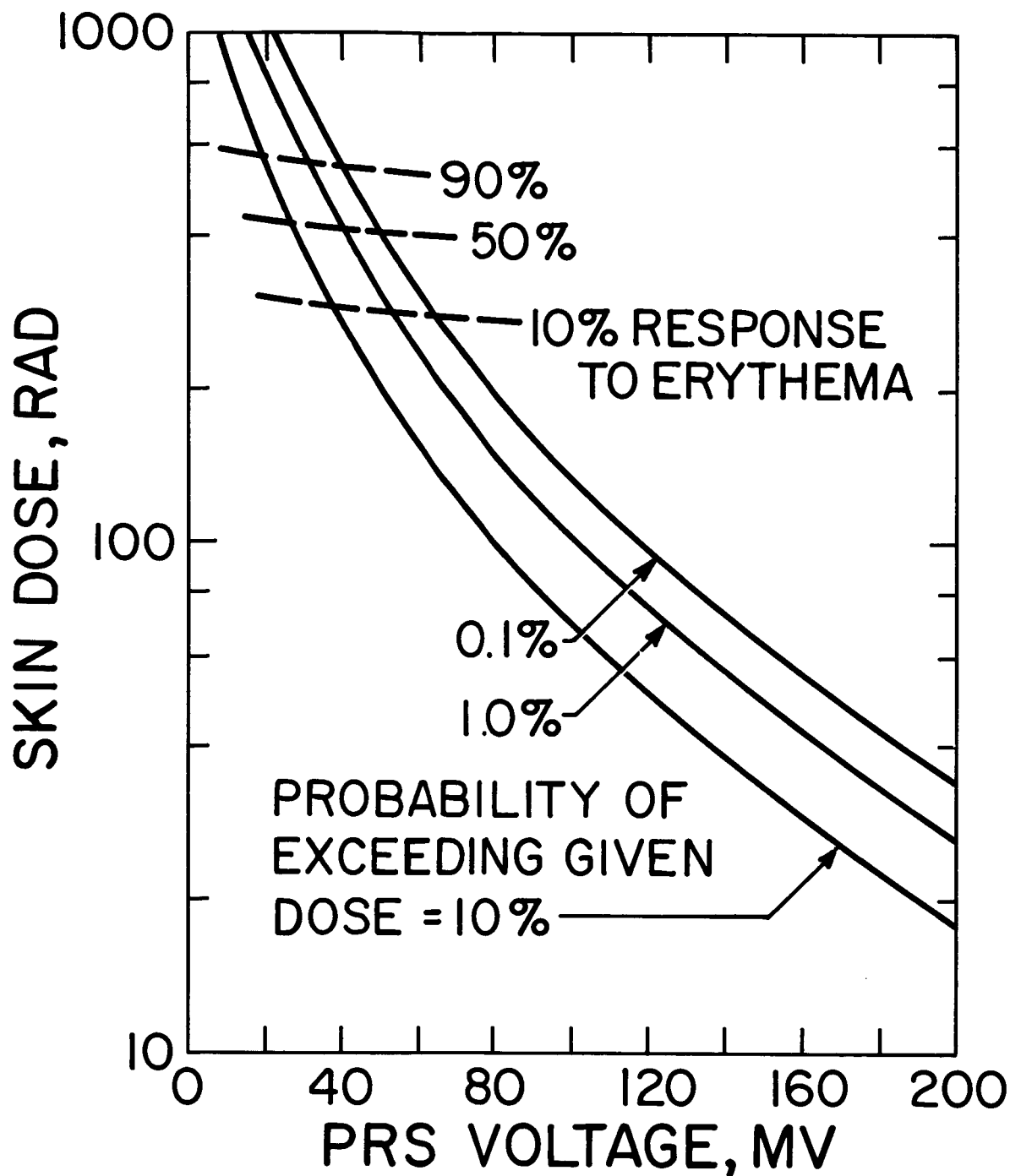
Fig. 6   Skin Dose vs PRS Voltage Required for Various Probabilities
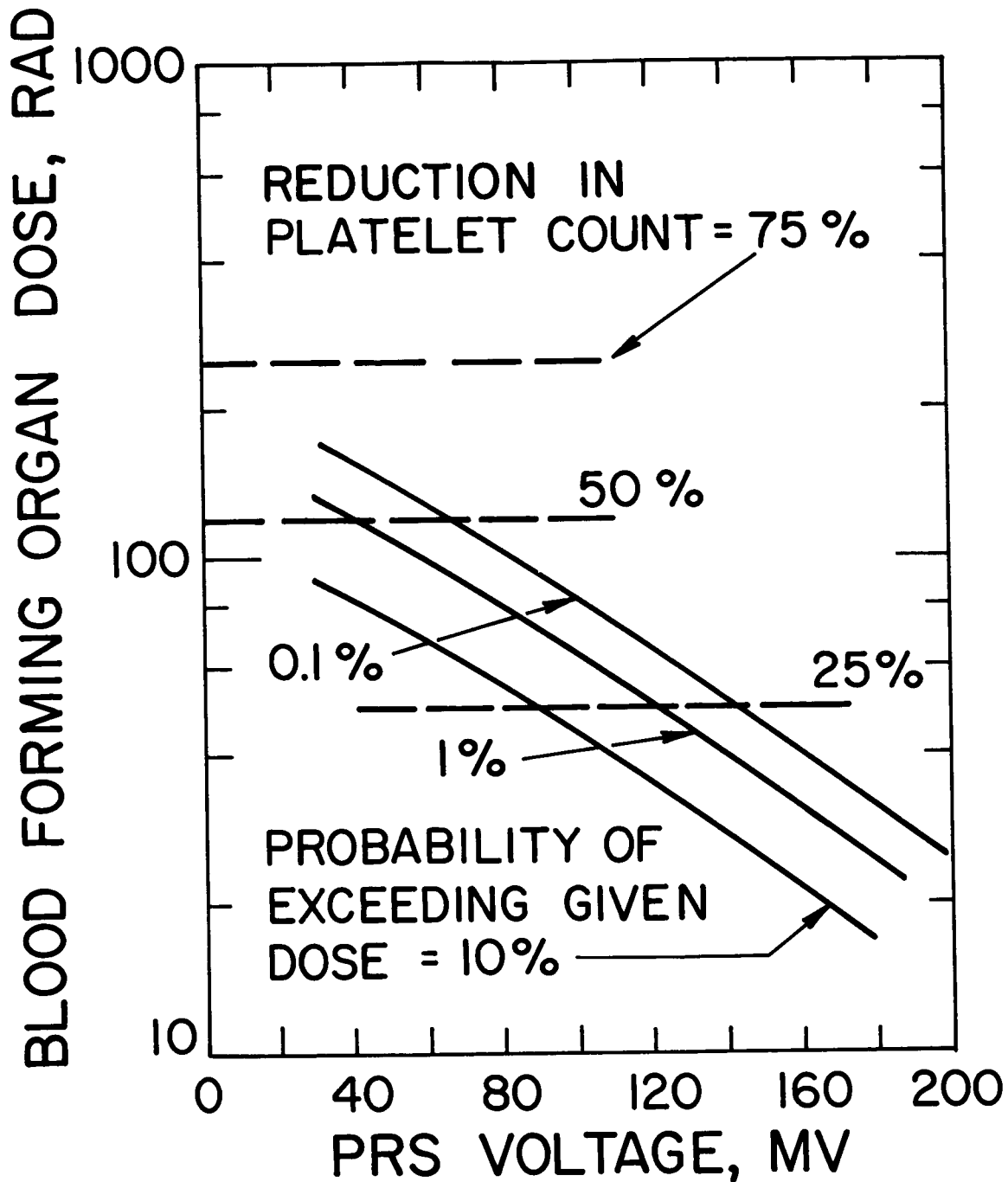   of Exceeding a Given Dose -- "Optimistic" Environment

Fig. 7   Blood-Forming Organ Dose vs PRS Voltage Required for Various Probabilities of Exceeding a Given Dose -- "Optimistic" Environment

III. RADIOBIOLOGICAL TOLERANCE CRITERIA

Introduction

In the previous section, the attenuation of the solar flare environment by means of passive and active shielding was considered, and results obtained of the severity of this environment (in terms of radiation dose) behind various amounts of shielding. In order to answer the basic question of the study, that of how much shielding is required on the mission, one must consider what are the maximum allowable radiation conditions to which the astronauts may be exposed. This section then is addressed to the problem of determining appropriate radiobiological tolerance criteria.

Somatic responses to ionizing radiations may manifest themselves in three time regimes:

1. Early effects that occur a few hours to a month after exposure,

2. Progressive effects that build up from chronic and acute exposures during a long flight,

3. Late effects that may occur long after the flight is over.

Early effects include skin responses such as erythema ("sunburn"), prodromal syndrome ("radiation sickness"), hematological responses (damage to blood-forming organs), early lethality, effects on the germinal epithelium (damage to gonads), etc. Early effects could incapacitate the spacecraft crew or degrade their performance, and could prove catastrophic if they occur during a crucial phase of the mission.

Continued exposure to a low level of radiation could result in a gradual build-up of hematopoietic injury. This injury will manifest itself in a general run-down condition of the crew, which could seriously compromise the reliable performance of their duties. Late effects such as general life shortening, leukemia, cataracts, etc., normally need not be considered (except for humanistic reasons) in mission planning since they normally would occur after the mission is over. (An exception to this might be missions to the outer planets where late effects could conceivably occur during latter portions of the flight). The present study will not consider late effects.

A factor that should be considered in formulating a radiobiological tolerance criterion is the demonstrated ability of the body to recover, at least in part, from earlier radiation damage. Because of this phenomenon, two exposures of radiation sustained several months apart are less damaging than one exposure of the same total dose. Also, under continuous exposure to a low level radiation, recovery and injury occur concurrently and it is

possible for an equilibrium to be maintained over long periods of time. Although there have been several attempts (eg. Refs. 4, 13) to quantify this phenomenon for use in mission planning, it is questionable whether the current body of knowledge on this subject allows this to be done with any real assurance. In addition, consideration of radiobiological recovery during a mission assumes a knowledge of the history of encounter with radiations during the mission. However, in the previous section it was seen that predicting the gross aspects (i. e., total dose, total flux, average spectra, etc.) of the radiation environment is difficult. It would therefore seem that predicting the detailed aspects (history of occurrence of flares, flux and spectrum of each flare, etc.) would be a hopelessly difficult task to carry out on any basis other than sheer guesswork. For these reasons, then, the recovery phenomenon was not considered in formulating the radiobiological tolerance criterion. (This phenomenon should not be confused with short-term rate effects, considered later).

It is further assumed in this section that the total or mission-integrated doses found in the previous section occur from one large flare (or sequence of flares in a time period of less than a week). This assumption leads to results that tend to err on the conservative side since fractionation would reduce the biological effects. The assumption is also not un-realistic since it has been shown by several authors (eg, Refs 9, 11) that during a large number of hypothetical missions, most of the dose results from one large flare. Because of this lack of knowledge of the time-phasing of solar flare exposures during the mission, it is not possible to make any evaluation of the progressive biological effects in this study. Instead, attention is focused on some critical early effects, namely skin effects and damage to the blood-forming system.

Damage Criteria

Because of the characteristics of solar flare spectra, when the astronauts are engaged in EVA or behind only a thin shield, a large propor-tion of the incident radiation is absorbed at or near their body's surface, i. e., the skin. Under suitable conditions, there will occur a sunburn-like reaction known as erythema in a few hours to a few days time after exposure. Larger doses will increase the severity of the erythema and result in other syndromes that are reminiscent of severe sunburns. The rubbing of the spacesuit against the affected areas will cause reactions that are at best annoying and at worst painful. In any case, the reaction will adversely affect the crew's efficiency and should be avoided.

The threshold for erythema response in individuals varies and Table 2 (from p. 247 of Ref. 14) presents values for absorbed dose of reference radiation to cause erythema in 10%, 50% and 90% of the population. The reference radiation is taken to be 200 to 250 kVp x-rays with a mean linear energy transfer (LET) of about 3.5 keV/μ, corresponding to a quality factor (QF) of one. The site of interest for this dose is taken as 0.1 mm below the surface, and the skin area exposed is 35 to 100 cm^2.

TABLE 2

Estimated Absorbed Dose Required to Produce Erythema (from Ref. 14)

Probability of Response	Dose (rad)
10%	400
50%	575
90%	750

The more energetic components of the solar flare spectra will penetrate a considerable distance into the body, even when it is protected by substantial shielding. Of particular importance is the absorption of these radiations by the blood-forming organs, located on an average of 4 or 5 cm below the body's surface. The consequent damage is manifested by changes in in the peripheral blood counts within from 1 to 10 days after exposure. Although it is difficult to relate hematological changes to specifics of mission performance degradation, it is generally agreed that a near-normal blood profile, as measured by the peripheral blood counts, must be maintained to ensure reliable performance of duties.

Of the blood-circulating elements the most sensitive to radiation are the platelets. The Table 3 (from p. 249 of Ref. 14) are values of absorbed dose of reference radiation at 5 cm depth that are required to depress the platelet count by 25%, 50% and 75%. The significance of these values for a space mission can be interpreted from the following "...a 25 percent depression of the circulating blood elements is indicative of early radiation damage to the blood-forming system. A depression of 75 percent and greater must be avoided, as it approaches the dosage range of probability of early radiation lethality."[14]

TABLE 3

Estimated Absorbed Dose Required to Depress Platelet Count
(from Ref. 14)

Reduction from Normal	Dose (rad)
25%	50
50%	120
75%	250

Factors that will modify the dose values in Tables 2 and 3 will be discussed in the following subsection.

Dose-Response Modifying Factors

Values of limiting dose given in Tables 2 and 3 cannot be applied directly to Figs. 2 and 3 to obtain shielding requirements since several factors that modify the dose-response relationship must first be considered. Discussion of these factors and the formulation of the problem is based on the exposition in Chapter 8 of Reference 14.

The dose-response relations typified by the values in Tables 2 and 3 are given in terms of absorbed dose of reference radiation under certain reference conditions. For radiations and conditions other than reference, such as in space exposures, certain multiplying factors must be applied. In the nomenclature of Ref. 14, this can be expressed as

$$RES \ (reu) = D \ (rads) \ x \ QF \ (f_1 \ x \ f_2 \ x. \ . \ . \ . \ f_n) \tag{8}$$

where RES is the reference equivalent space exposure, reu are reference equivalent units, D is the space radiation dose, QF is the quality factor that accounts for differences in LET-dependence or radiation quality between the reference and space rediations, and f_1, f_2. . . . f_n are factors that account for differences in space and reference exposure conditions. It might be noted that in an earlier notation, dose equivalent was analogous to RES, rem to reu, and RBE to QF. Application of Eq. (8) is as follows: a certain dose D of space radiations is absorbed at the site of interest under given space exposure conditions. Appropriate values of QF, f_1, f_2. . . f_n are used in Eq. (8) to calculate RES. Assuming 1 reu is equivalent in biological risk to 1 rad of reference radiation, the resulting RES value is used to determine the biological response from Tables 2 and 3.

For a given response to a given type of monoenergetic radiation, QF depends (in general) on the LET value, which in turn is a function of the energy of this radiation, The case of interest here, however, is the spectrum of energies that exists inside the spacecraft at the time of a solar flare. In this case, the effective QF is some function of the interior energy spectrum, which, in turn, depends on the amount and type of shielding. Therefore, the average or effective QF is some function of the shielding parameters. As pointed out in Ref. 14, QF values also depend on whether early or late effects are being considered. For early skin responses, Table 5 of Ref. 14 suggests the following QF values for monoenergetic radiations:

$$low \quad LET \quad (\lesssim 3.5 \ keV/\mu), \ QF = 1$$

$$high \quad LET \quad (>3.5 \ keV/\mu), \ QF = 3$$

For protons, an LET = 3.5 keV/μ corresponds to a proton energy of about 10 MeV.[15]

For a given solar flare spectrum, transport calculations can be used to obtain the spectrum inside a stipulated thickness of aluminum or PRS voltage. The conditions that QF = 1 for energies greater than or equal to 10 MeV and QF = 3 for energies less than 10 MeV can then be used to calculate an average QF. This was done for a spectrum that had a characteristic rigidity of 100 MV (a value close to the mean value of 97 MV for Solar Cycle 19 flares[11]), and for various thicknesses of aluminum and PRS voltages. Results in terms of average QF vs aluminum shield thickness and PRS voltage are shown in Figs. 8a and 8b.

For the case of the early hematological response, the same reference recommends use of a QF = 1, independent of LET value (and therefore independent of shield thickness or voltage).

The other factors in Eq. (8), f_1, f_2.....f_n, account for differences between space and reference exposure conditions. Some of these may be spatial non-uniformities in depth, area, volume, etc. exposed. For instance, the early hematological response depends on the body volume, and hence the amount of bone marrow, exposed. The values given in Table 3 were for a volume exposure of at least as large as the trunk; if only the extremities are exposed, the volume factor, f_v, might be 1/5.[14] For the analysis of this study, it will be assumed that the whole body is exposed so that f_v = 1 for the hematological response case. It will be remembered that the values in Table 2 were for exposed skin areas of 35 to 100 cm^2. The early skin responses are somewhat area-dependent and for a whole-body exposure it is recommeded[14] that the area factor, f_a, be taken as 1.25. Since the calculated space doses are for the same body depths as those listed in Tables 2 and 3, the penetration factor, f_p, may be taken as unity for both responses of interest.

As was discussed previously, rate effects can have a significant effect on the response. Reference 14 suggests taking this phenomenon into account through the use of a rate-effectiveness factor, f_r. For early hematological response, the exposure is most effective if it is spread over 1 or 2 days or less; reduction in effectiveness is only obtained if the dose is protracted over several weeks. Since the duration of the average solar flare is about 1 or 2 days, this suggests that a f_r value of unity is appropriate for this response. On the other hand, for early skin responses, the exposure is most effective if the dose is delivered over 1 or 2 hours or less; if the dose is spread over 4 to 6 days or longer, the effectiveness is reduced by a factor of 3 (f_r = 1/3). Some sequences of solar flare events (eg. July 1959, Novermber 1960) are spread over this range of time durations but the average flare lasts only 1 or 2 days. Taking this into account, a somewhat lower value of f_r might be appropriate in the present context, for instance f_r = 1/2.

Fig. 8a   Quality Factor vs Amount of Shielding
100 Mv Rigidity Spectrum
QF = 1 for LET $\leq$ 3.5 keV/μ
QF = 3 for LET $>$ 3.5 keV/μ

(a) Passive Shield

B 3023
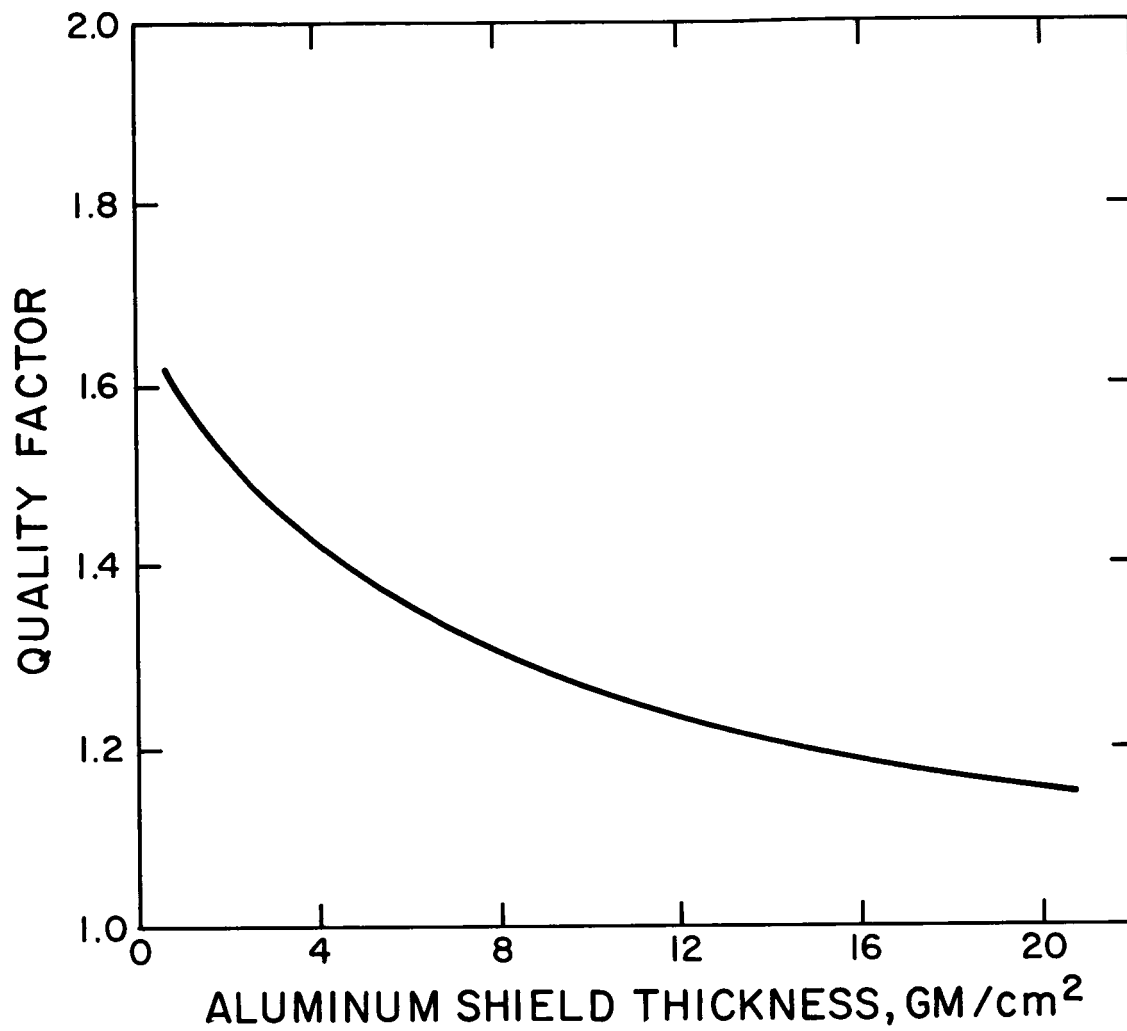
Fig. 8b   Quality Factor vs Amount of Shielding
100 Mv Rigidity Spectrum
QF = 1 for LET $\leq$ 3.5 keV/μ
QF = 3 for LET > 3.5 keV/μ

(b) PRS Shield
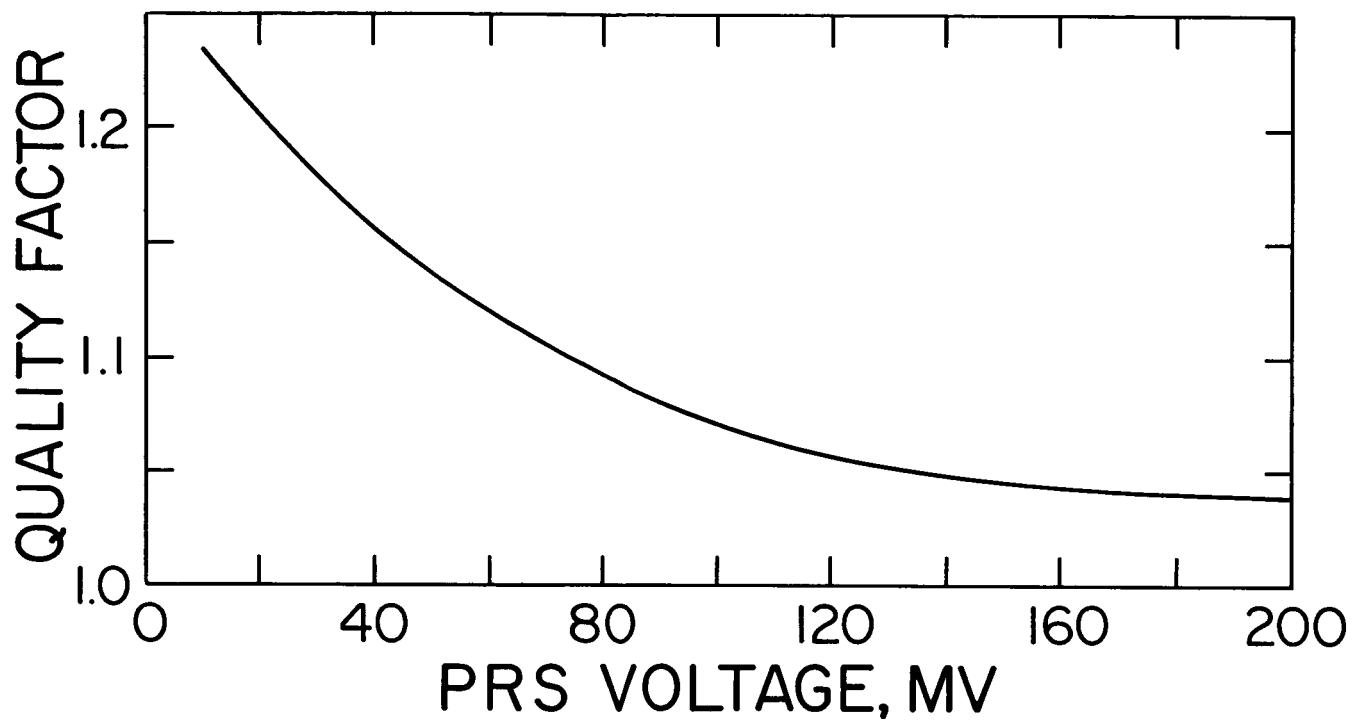
Radiation recovery rates are a function of the LET values (of the incident radiation), with the greatest recovery rates being associated with low LET radiations. The values of f_r given above are actually for the low LET omponents of the incident radiation; for the high LET components, it may be assumed that no recovery takes place and $f_r = 1$. A borderline value between high and low LET radiations of 15 keV/μ is suggested in Ref. 14; this corresponds[15] to an energy of about 2 MeV. Because of this dependence of f_r on LET, for a given flare spectrum f_r is again a function of shield thickness or voltage. However, the percent of dose that is delivered by radiations with energies less than 2 MeV is small, except possible behind very thin or low voltage shields. Therefore, it would seem justified to neglect the LET-dependence of f_r for cases of practical interest, and take the above values of f_r for the entire spectrum.

In summary, the modifying factors in Eq. (8) for early skin response and early hematological response can be tabulated as follows:

Early Skin Response:

QF = QF(X) where, for a 100 Mv spectrum QF is given in Figs. 8a and 8b (X = shield thickness or PRS voltage).

and

$$f_p = 1, \quad f_a = 1.25, \quad f_r = 0.5$$

Therefore, $(RES)_{Skin} = 0.63 \times QF(X) \times D$ \hfill (9)

Early Hematological Response:

$$QF = 1, \quad f_p = 1, \quad f_v = 1, \quad f_r = 1$$

Therefore, $(RES)_{Hemo.} = D$ (independent of shield thickness or voltage) \hfill (10)

Discussion

The multipliers of D in Eqs. (9) and (10) may be considered as factors by which the ordinate values of the curves in Figs. 2 through 7 must be multiplied in order to compare the space doses with the allowable reference doses given in Table 2 and 3. This factor is, of course, unity in Eq. (10) but in Eq. (9) it varies (for passive shielding) from 1.0 at X = 1 gm/cm2 Al, to 0.72 at X = 20, to 0.63 for very large values of X. A similar (but smaller) variation with voltage may be observed for active shielding. Rather than replotting the skin dose curves to account for this variable factor, a simple but less physically-meaningful procedure is

adopted of dividing the values in Table 2 by this factor and plotting the result in Figs. 2, 4, and 6. The absorbed doses required to depress the platelet count (from Table 3) are superimposed on the curves of Figs. 3, 5 and 7.

It is of interest to compare the radiobiological tolerance criteria for early skin and hematological responses as given by Tables 2 and 3, respectively, with similar criteria suggested by other authors. In regard to the former response, Ballinger[16] indicates that about 200 to 300 rad is the threshold for observation of early erythema. He also indicates that the body can repair from skin doses of from 400 to 600 rad, but that skin doses above 500 rad produce certain degrees of performance decrement. Reference 17 (p. 43) suggests that a mild erythema will be produced following an acute dose of 650 to 700 rem (460 to 500 rad with an RBE = 1.4) at the depth of the basal layer of the skin; and severe damage, and perhaps even death, will occur at doses of 1800 to 2000 rem. Billingham,[18] in discussing Apollo dose limits, suggests an RBE value for the skin response of 1.4 with an average yearly skin dose of 250 rad (350 rem), and a maximum permissible single acute emergency exposure of 500 rad (700 rem. In summary, then, it can be seen that the values presented in Table 2 are at least in reasonable agreement with similar values suggested by other authors; an acute dose of 400 rad is probably acceptable as it represents either a very mild erythema response in most people or a somewhat more severe, but not incapacitating, response in about 10% of the population. On the other hand, an acute dose of 750 rad should probably be avoided as it is liable to cause a severe reaction in a considerable portion of the population or a mild response in almost all the population.

In regard to early hematological response, Billingham[18] suggests an RBE value of 1.0 with an average yearly dose to the blood-forming organs of 55 rad, and a maximum permissible single acute emergency exposure of 200 rad. Reference 17 indicates that at a dose level of 150 to 200 rem (= rad), symptoms can reach a clinically aggravated level within a few days to three weeks after exposure. These results generally corroborate the values in Table 3 and indicate that while a blood-forming organ dose of 50 rad is probably acceptable, 250 rad probably is not.

IV. RESULTS

The curves of dose vs shield thickness as presented in Figs. 2 through 7 have wide applicability in that one may select allowable values of skin and blood-forming organ dose, as well as an appropriate probability of exceeding that dose level, and calculate the necessary shielding thickness or voltage as per the environment predicted by his favorite author. However, in this section some specific values of dose and probability parameters will be suggested, and resulting shielding requirements will be obtained and compared.

Although it is not the intent of this paper to promulgate still another mission radiation exposure criterion for manned space flight, the results of the previous section do suggest several approaches for doing so. One approach might be to allow a very low probability of exceeding a dose value that corresponds to significant radiobiological damage. This probability could be made commensurate with that for the occurrence of other comparable spacecraft system failure mechanisms --eg., the probability of the penetration of the spacecraft wall by large meteorite. This approach might lead to a criterion of, for instance, 0.1% probability of exceeding 750 rad to the skin or 250 rad to the blood-forming organs. (For brevity in the following discussion, this will be designated Criterion A). Another approach might be to allow a higher probability of exceeding a dose level that corresponds to less critical, or even threshold, radiobiological damage. For instance, the resulting criterion might be 10% probability of exceeding 400 rad to the skin and 50 rad to the blood-forming organs (Criterion B). This second approach, while leading to generally less stringent shielding requirements than the first, is subject to somewhat more uncertainties and/or imponderables. For instance, what could be an unimportant response during 95% of the mission time may mean the difference between success and failure if it occurs during a crucial phase of the flight when the crew members must be possessed of all their faculties. Also, synergistic effects with other space environmental factors may turn a normally-acceptable response into an unacceptable response. In the subsequent paragraphs, both criteria will be utilized to obtain shielding requirements.

When Criterion A is used in conjunction with Figs. 2a and 3a, and Criterion B with Figs. 2c and 3c, the range of passive shielding requirements shown in Table 4 result. Of a given set of 2 values in Table 4, the first value corresponds to the pessimistic, and the second to the optimistic environment predictions.

TABLE 4

Ranges of Passive Shielding Requirements

Criterion	Shielding Required, $gm/cm^2 Al$	
	skin damage	BFO damage
A	22 (Ref. 11) to 4 (Ref. 8)	35 (Ref. 11 to 6 Ref. 10)
B	5 (Ref. 11) to 3 (Ref. 7)	15 (Ref. 11 to 9 (Ref. 7)

Several important conclusions can be drawn from the results of Table 4. First, for the examples chosen, damage to the blood-forming organs is more critical than damage to the skin (in that the former requires a greater amount of shielding). This is valid for both criteria when comparing corresponding values for both the pessimistic and optimistic environments. Second, for the pessimistic environments, there is a very large difference in shielding requirements resulting from use of Criterion A as compared with Criterion B. Although this difference is most significant in the case of skin damage, there is also a factor of 2 difference in BFO damage. Because of these large differences, it would seem necessary to give considerable thought in mission planning to the stipulation of the mission radiation exposure criterion. For the optimistic environment, this difference is much smaller.

It is of some interest to compare the results in Table 4 with the results that would be obtained if an analogous mission exposure criterion as proposed by the AIAA Spacecraft Technical Committee[19] were used. In this paper, it is suggested that a 1% probability of exceeding 50 rad to the blood-forming organs and a 0.1% probability of exceeding 220 rad to the body midplane (11 cm depth) be the determining criterion. While the data in this report do not allow determination of the shielding requirements on the latter basis, they do on the former basis. Figure 3b then yields a range of from roughly 50 gm/cm^2 (Ref. 11) for the pessimistic environment, to 13 gm/cm^2 (ref. 7) for the optimistic environment.

It should be remembered that the shielding thicknesses derived in this section are for an aluminum shield. Considerable weight savings, on the order of 30% to 40%, could be attained if a more efficient shielding material, such as polyethylene, were used.

Analogous to Table 4, a similar table can be drawn up to show the range of required PRS voltages. Using the mission radiation exposure criteria previously discussed, together with the curves of Figs. 4 through 7, Table 5 results.

TABLE 5

Ranges of Active (PRS) Shielding Requirements

Criterion	Shielding Required, MV	
	skin damage	BFO damage
A	128 to 39	129 to < 20
B	53 to 37	88 to 54

In Table 5, the first value in each set of 2 corresponds to a pessimistic environment prediction (as given by an analysis similar to that in Ref. 11), and the second to an optimistic environment prediction (as given by an analysis similar to that in Ref. 10). Thus the results for the pessimistic environment in Table 5 are generally comparable to similar values in Table 4, while those for the optimistic environment are not.

As in the case for passive shielding, for the pessimistic environment, the requirements for shielding are more severe with Criterion A as opposed to Criterion B. On the other hand, as contrasted to the case for passive shielding, for the pessimistic environment the requirements on shielding to prevent skin and blood-forming organ damage are about the same. Also, in Table 5, it is seen that in 3 out of 4 cases the pessimistic environment requires a higher shielding voltage than does the optimistic environment.

It is instructive to compare the shielding requirements for passive and active systems that were obtained using the same assumptions as to environment, biological response, and mission radiation exposure criterion. This comparison can be made between the corresponding pessimistic environment values in Tables 4 and 5. One way of effecting such a comparison is to note that since a PRS of voltage V MV would repel all protons of energy less than V MeV, the PRS is in a sense "equivalent" to an aluminum shield with thickness that would just stop a proton of this energy. If the pessimistic environment voltages in Table 5 are converted to gm/cm^2 of aluminum on this basis, it is found that these values are substantially lower than the counter-part values in Table 4. The difference is particularly noticeable at the higher voltages. For example, for skin damage and Criterion A, 128

MV becomes 15 gm/cm^2 Al as compared to 22 gm/cm^2 in Table 4; for BFO damage and Criterion A, 129 MV becomes 15 gm/cm^2 as compared to 35 gm/cm^2 in Table 4. These differences are probably due to two factors. First, for skin damage, the scattering phenomenon discussed in connection with Eq. (6) acts to dispose of a large number of low energy, high LET protons. The scattering thus also causes a reduction in average QF for skin damage (see Figs. 8a and 8b). For BFO damage, the scattering probably is less important in reducing the dose. The enhanced effectiveness of the PRS in this case is probably due to greater efficacy of the PRS against the high energy, deeply-penetrating protons. For example, for a 130 MeV proton, a 100 MV PRS will reduce its energy to 30 MeV, while an "equivalent" aluminum shield of 10 gm/cm^2 will reduce its energy to 75 MeV. In this example the proton would not penetrate to BFO depth in the former case while it would in the latter.

The rate of loss of energy of fast particles in matter is a strongly decreasing function of energy so that a passive shield becomes increasingly less effective as the energy of the incident protons increases. At these energies, a PRS appears superior to a passive shield, as shown in the above example. On the other hand, at low energies, a passive shield is relatively effective. These considerations lead one to examine the possibility of a hybrid shield that would combine the effectiveness of a PRS against high energy particles with the effectiveness of a passive shield against low energy particles. Some, if not all, of the passive shielding would be provided by the structural shell of the spacecraft, which typically is about 2 gm/cm^2 aluminum. Thus a hybrid shield that utilizes the vehicle's shell and is "equivalent" to 10 gm/cm^2 aluminum passive shield, would require a 60 MV PRS (located exterior to the shell) to stop a 100 MeV proton. Against protons of energy higher than 100 MeV, the hybrid shield is more effective than the passive shield. For instance, a 130 MeV proton would be slowed to 75 MeV by the 10 gm/cm^2 passive shield. With the 60 MV, 2 gm/cm^2 "equivalent" hybrid shield, the 130 MeV proton is slowed to 54 MeV. Other examples of hybrid combinations, and comparisons with purely passive systems, may be found in Refs. 1 and 20. These comparisons show that hybrid systems remove more energy from incident protons than do "equivalent" passive systems. Because of this enhanced efficacy, and because a certain amount of passive shielding is inherent in any spacecraft, the hybrid shielding concept appears very attractive and warrants further investigation.

One general conclusion that may be drawn from the investigation is that the role of judgment in determining the necessary amounts of radiation shielding should not be undersold. This factor is of considerable importance in postulating the radiation environment that can be expected on future flights, as well as in the setting of allowable somatic damage levels and acceptable probabilities of exceeding these levels.

REFERENCES

1. Levy, R. H. and Janes, G. S., "Plasma Radiation Shielding," AIAA Journal, v. 2, no. 10, October 1964, pp. 1835-1838.

2. Levy, R. H. and French, F. W., "Plasma Radiation Shield: Concept and Applications to Space Vehicles," 13th Annual Mtg. of Am. Nuclear Soc., San Diego, Calif., June 11-15, 1967, contained in NASA SP-169, 1968; see also J. S. R., v. 5, no. 5, May 1968, pp. 570-577.

3. French. F. W., "Radiation Shielding of Manned Mars Vehicles," AIAA/AAS Stepping Stones to Mars Meeting, Baltimore, Maryland, March 28-30, 1966.

4. French, F. W., and Hansen, K. F., "Radiation Shielding Requirements for Manned Satellites," J. S. R., v. 2, no. 6, pp. 931-937, 1965.

5. Curtis, S. B. and Wilkinson, M. C., "Study of Radiation Hazards to Man on Extended Missions," NASA CR-1037, May 1968.

6. Modisette, J. L., Snyder, J. W., Juday, R. D., "Engineering Models of the Space Radiation Environment," 13th Annual Mtg. of Am. Nuclear Soc., San Diego, Calif., June 11-15, 1967, contained in NASA SP-169, 1968.

7. Webber, W. R., "An Evaluation of the Radiation Hazard due to Solar-Particle Events," Boeing Co. Report D2-90469, December 1963.

8. Burrell, M. O., Wright, J. J., and Watts, J. W., "An Analysis of Energetic Space Radiation and Dose Rates," NASA TN D-4404, February 1968.

9. Snyder, J. W., "Radiation Hazard to Man from Solar Proton Events," J. S. R., v. 4, no. 6, pp. 826-828, 1967.

10. Hilberg, R. H., "Radiation Shielding Needed for Extended Interplanetary Missions - Case 103-2," Bellcomm Memo, August 11, 1966.

11. Modisette, J. L., Vinson, T. M., Hardy, A. C., "Model Solar Proton Environments for Manned Spacecraft Designs," NASA TN D-2746, April 1965.

12. North American Rockwell Corp., "Technological Requirements Common to Manned Planetary Missions, Appendix B, Environments," Report SD 67-621-3, January 1968.

13. Baum, S. J., "Recommended Ionizing Radiation Exposures for Early Exploratory Space Missions," Aerospace Medicine, v. 33, no. 10, October 1962.

14. Langham, W. H., ed., "Radiobiological Factors in Manned Space Flight," Report of the Space Radiation Study Panel of the Life Sciences Committee, Space Science Board, National Academy of Sciences, National Research Council, NAS/NRC Publication 1487, 1967.

15. Schaefer, H. J., "Dosimetry of Proton Radiation in Space," U. S. Naval School of Aviation Medicine, Pensacola, Fla., Report No. 19, 1961.

16. Ballinger, E. R., "Status of Research to Determine Radiobiological Response Criteria for Space Missions," 13th Annual Mtg. of Am. Nuclear Soc., San Diego, Calif., June 11-15, 1967, contained in NASA SP-169, 1968.

17. "Radiation Biology and Space Environmental Parameters in Manned Spacecraft Design and Operation," Aerospace Medicine, v. 36, no. 2, Section 11, February 1965.

18. Billingham, J., "Status Report on the Space Radiation Effects on the Apollo Mission -- Apollo Dose Limits," Second Symp. on Protection Against Radiations in Space. Gatlinburg, Tenn., Oct. 12-14, 1964; contained in NASA SP-71, 1965.

19. Jenkins, L. E. and Spacecraft Committee of AIAA, "Spacecraft Requirements for Manned Planetary Missions," AIAA Technology for Manned Planetary Missions Mtg., New Orleans, La., March 4-6, 1968.

20. Shelton, R. D., Watts, J. R., and Stern, H. E., "Advantages of Using a Combination Electromagnetic and Material Shield," to be published.